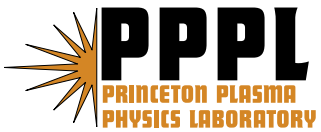

Princeton Plasma Physics Laboratory

PPPL-

PPPL-



Prepared for the U.S. Department of Energy under Contract DE-AC02-09CH11466.

Princeton Plasma Physics Laboratory

Report Disclaimers

Full Legal Disclaimer

This report was prepared as an account of work sponsored by an agency of the United States Government. Neither the United States Government nor any agency thereof, nor any of their employees, nor any of their contractors, subcontractors or their employees, makes any warranty, express or implied, or assumes any legal liability or responsibility for the accuracy, completeness, or any third party's use or the results of such use of any information, apparatus, product, or process disclosed, or represents that its use would not infringe privately owned rights. Reference herein to any specific commercial product, process, or service by trade name, trademark, manufacturer, or otherwise, does not necessarily constitute or imply its endorsement, recommendation, or favoring by the United States Government or any agency thereof or its contractors or subcontractors. The views and opinions of authors expressed herein do not necessarily state or reflect those of the United States Government or any agency thereof.

Trademark Disclaimer

Reference herein to any specific commercial product, process, or service by trade name, trademark, manufacturer, or otherwise, does not necessarily constitute or imply its endorsement, recommendation, or favoring by the United States Government or any agency thereof or its contractors or subcontractors.

PPPL Report Availability

Princeton Plasma Physics Laboratory:

<http://www.pppl.gov/techreports.cfm>

Office of Scientific and Technical Information (OSTI):

<http://www.osti.gov/bridge>

Related Links:

[U.S. Department of Energy](#)

[Office of Scientific and Technical Information](#)

[Fusion Links](#)

DIGITAL COIL PROTECTION SYSTEM (DCPS) ALGORITHMS FOR THE NSTX CENTERSTACK UPGRADE

R. D. Woolley,
P. H. Titus, C.L. Neumeyer, R. E. Hatcher

Princeton Plasma Physics Laboratory,
Princeton, NJ 08543-0451
woolley@pppl.gov

Abstract—A significant upgrade is planned for the National Spherical Torus eXperiment (NSTX) in which plasma current and confining magnetic field intensities will nearly double while plasma duration will more than double. Changes will include replacing the existing centerstack with a new one containing a thicker TF inner Leg, a new OH solenoid coil, and an expansion to six of the complement of PF1 coils controlling plasma divertor shape. Other coils will remain in service with hardware modifications as needed for their approximately three-fold increases in magnetic forces.

The new Digital Coil Protection System (DCPS) will avoid the costly need to further upgrade coils and their mechanical supports to withstand control misoperations that could otherwise take them well beyond the operating envelope of critical variables (i.e., forces, stresses and temperatures) actually needed for the new regime of plasma experiments. This improvement would be impossible using the present protective scheme of independent overcurrent trips for each coil circuit which ignores effects of current combinations. In the upgraded NSTX, the DCPS will operate on a fixed cyclic repetition rate fast enough to avoid latency issues, e.g., 1 millisecond, monitoring currents in the plasma, in the OH solenoid coil, in 12 PF coil circuits, and in the TF coil. Its algorithms will calculate in real time the present and projected maximum future values of each critical variable that would be reached if protective action were commanded now, with and without a full plasma disruption event. The DCPS will command the protective action to begin if any such calculated critical value exceeds its operating limit; power supplies are then bypassed by applying zero volts to coil circuit terminals.

*This work supported by the US DOE Contract No. DE-AC02-09CH11466

Keywords- coils; protection; equipment safety

I. INTRODUCTION

All significant magnetic fusion research facilities have features to protect their investments in magnetic field coils. Such features can be divided into two different categories. One is focused on the mitigation of coil circuit failure events such as insulation failures, ground faults, shorted turn faults, etc. The second is focused on the enforcement of critical variable operating limits intended to avoid failures in the coil system or its supporting structures. The Digital Coil Protection System (DCPS) is devoted entirely to the second category, enforcement of operating limits in the absence of a coil system fault.

It is not reasonable to base coil protection on the checking in advance of plans for an experiment, since actual pulses can profoundly deviate from their plans. E.g., any deviation of

injected gas or of auxiliary heating power from prior plans causes coil currents to deviate. It also is not practical to directly measure critical variables due to their sheer number, instrumentation expense, noise, and failure modes introduced.

Operating limits enforced by the DCPS are on critical variables which depend on coil currents. For these, a reduction of coil currents to zero reduces the risk of failure. Coil operating limits exist on (1)temperatures of coil conductors and insulation, (2)magnetic Lorentz forces on coils and their structural supports, and (3)mechanical stresses in coils or their supports depending on temperatures and/or Lorentz forces.

The DCPS is simple, robust, and secure. To avoid compromise by unreliable inputs it will receive no advance warning of a pulse from the controls computer, no timing signals, nor will it have any table of standard scenarios. To avoid compromising equipment safety by ill-advised modifications it will be kept off the local network thus preventing unauthorized changes. Its output will command a reliable hard shutdown to occur rather than a soft control action which may not work. (If needed, the DCPS could warn the control computer recommending soft shutdown.)

II. BLOCK DIAGRAM

A simplified block diagram of the DCPS is shown in Fig.1. The DCPS operates continually at all times, repeating its equipment-protective safety algorithms once per millisecond. Its operation is not suspended with the cycling of the NSTX device; instead it is always active whenever the power conversion system is not entirely disabled and powered down.

Process signals monitored each millisecond by the DCPS include coil and plasma currents, supplied coolant temperature and pressure at the header supplying coils, and coolant flow status. The DCPS algorithms calculate critical variable values, decide whether operating limit violation is imminent, and if so issue a latching shutdown command for the coil power system to reliably transition the coil currents to a safe shutdown condition. Separate equipment within the coil power system's hardwired safety controls implements that transition.

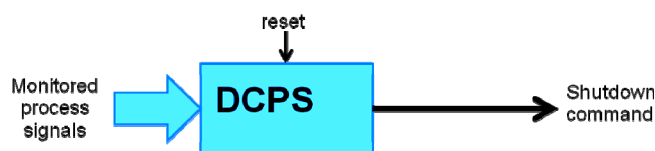


Figure 1: Digital Coil Protection System (DCPS) Block Diagram

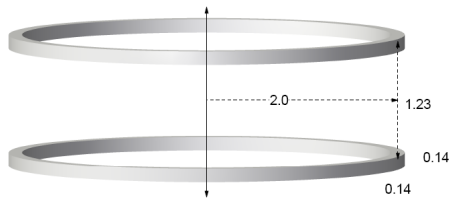


Figure 2: Two Coaxial Coils

III. COMPLEXITY OF SAFE OPERATING REGION

To illustrate the motive for including the DCPS as part of the planned NSTX centerstack upgrade, consider the following simplified analogy of two coaxial coils, each 24 turn, 4m diameter, 1.23m separation, as shown in Fig.2. With each coil having its own independently controllable current, I_1 and I_2 , the force between the coils is proportional to the product of their currents and varies over the 2D space of possible current combinations as shown in the Fig.3 contour plot. Hoop tensions in the coils vary as in the Figs.4 and 5 contour plots.

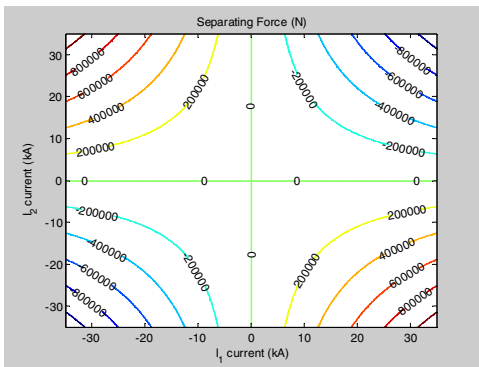


Figure 3: Separating Force Between Coils

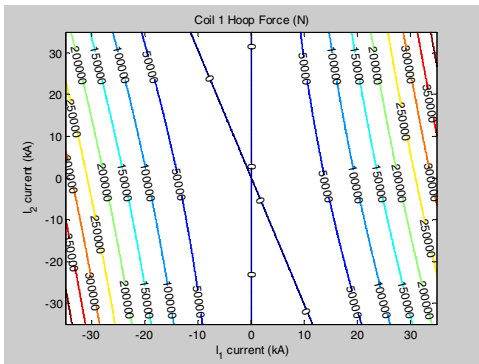


Figure 4: Hoop Force in Coil 1

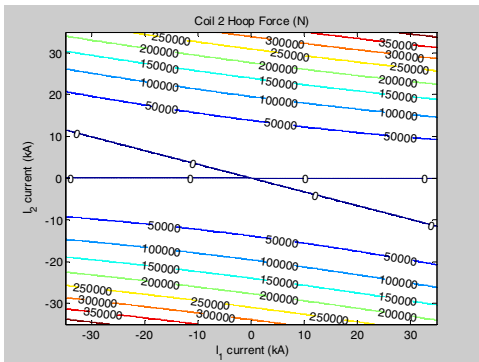


Figure 5: Hoop Force in Coil 2

Operating limits of 200 kN on the absolute intercoil force and on each of the two absolute hoop forces can be traced as the intersection of contour-limited regions from Figs. 3-5; they would leave the allowable operating region in current space shown in Fig.6. Operation anywhere within this region of complex shape can be safely allowed by a digital coil protection system enforcing these force operating limits. However, a simpler system that separately limits each current magnitude independent of the others would need to restrict operation to the much smaller square region shown in Fig.7, in which strong magnetic field combinations cannot be obtained.

NSTX has 14 independently variable coil currents plus the plasma current, so would need a plot in 15 dimensions to similarly show its allowable operating region. Such plots are impossible to visualize and impractical to even store. However, the principle from the 2D analogy remains that single-current limits do not fit well to the shapes of safe operating regions. Single-current limits can prevent operating limit violations but only by wastefully abandoning otherwise safe operations at high current. For the NSTX centerstack upgrade whose purpose is to allow operation at higher currents, this is the main reason for implementing the DCPS.

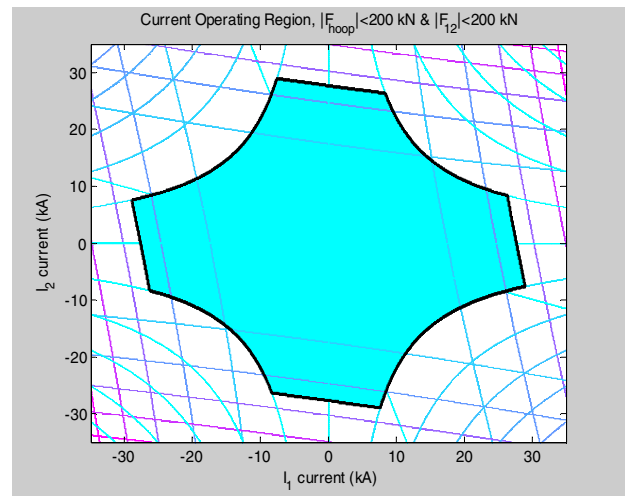


Figure 6: Safe Operating Region with Forces Less than 200 kN

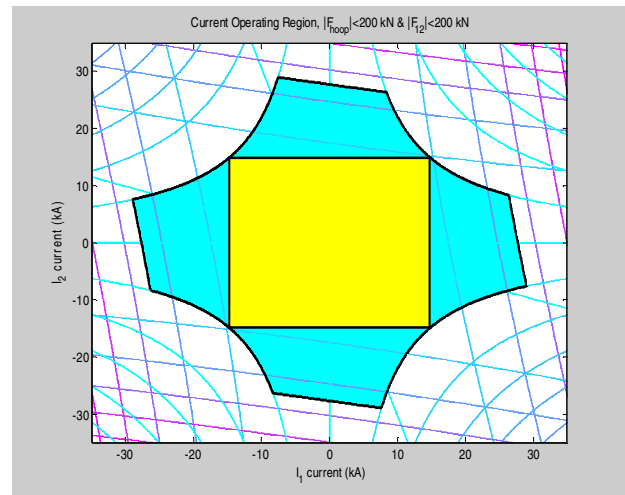


Figure 7: Safe Operating Square Region with Single Current Limits

IV. CRITICAL VARIABLE ALGORITHMS

Critical variables can be estimated in real-time from the known distribution of currents and from coil coolant temperature and pressure which determine coil cooling rates. Magnetic field strength operating limits would be important for quench avoidance in tokamaks with superconducting coils. The field anywhere can be evaluated as the following sum:

$$\vec{B}(\vec{r}_i) = \sum_{j=1}^n \vec{b}_{ij} I_j \quad (1)$$

The I_j are currents and the \vec{b}_{ij} are coefficients calculated for location i . Since NSTX coils are resistive Eq.(1) is not used in the DCPS. However, magnetic field is related to Lorentz forces which are important. Total integrated force on a coil is a multivariable quadratic function of currents as follows:

$$F_i = I_i \sum_{j=1}^n a_{ij} I_j \quad (2)$$

Here F_i is the magnetic Lorentz force on coil i , I_i is the current in coil number i , I_j is the same as in Eq.(1), and a_{ij} is a table of force influence coefficients for the coils and plasma. Note that coil geometry is fixed so force influence coefficients for the coil currents are also fixed. Plasma geometry can change somewhat within the spatial envelope allowed by vacuum vessel structures, so values of the true plasma current force influence coefficients could change some but can be approximated by fixed values. Using precalculated force influence coefficients and real time current measurements, a digital computer can evaluate Eq.(2) extremely fast, calculating in real time the forces on coils.

Coil temperatures change according to time-dependent differential equations modeling heating and cooling processes. These can be numerically updated in real time by a dedicated digital computer using precalculated coefficients with real time measurements of coil currents, coil coolant inlet temperature and header pressures. Joule heating varies as the square of coil current times the local temperature-dependant copper resistivity which itself can be determined at multiple internal locations within a coil from simulated local temperatures.

Simulated coolant temperatures within a coil are used to interpolate coolant viscosities which are combined with the measured pressure drop between supply and return headers and flow calibration test data to track the coolant flow rate, which in turn is used with measured coolant inlet temperature to advance the thermal model by transferring heat from copper to coolant and moving the coolant downstream. (Note that any coolant blockages are detected by separate flow monitoring "switches" interlocked to prevent operation of uncooled coils.)

For materials operating within elastic ranges, stresses are linear with spatial distributions of force and temperature loadings so mechanical stress components can be calculated in real time using the following algorithm:

$$\sigma_\ell(\vec{r}_i) = \sum_{j \leq k} c_{ijk\ell} I_j I_k + \sum_{m=1}^n d_{i\ell m} T_m \quad (3)$$

Here, the subscript i denotes the i^{th} location for stress component evaluation, ℓ denotes a particular stress component at that location, while the j, k indices refer to the different currents flowing in coils, other metallic components, or plasma. All of these c and d coefficients can be determined in advance from sophisticated analyses of the stress distributions caused by combined thermal and electromagnetic loadings [1]. The coefficients can be extracted from finite element models by judiciously choosing unit loading conditions and linearly combining the calculated stresses from different loading cases as needed. The resulting coefficients can be stored in numerical tables. The Eq. (3) algorithm can then be evaluated extremely fast by a digital computer using real time measurements of currents along with temperatures simulated via the real time measurements previously described. It should be noted that for accuracy of this algorithm the finite set of temperatures must be chosen with sufficient degrees of freedom to approximate the spatial variations of temperatures that can actually occur.

V. PROTECTIVE ACTION AND ITS AFTERMATH

Just as a driver should hit the brakes far enough before actually hitting a deer to allow for the estimated braking distance, so should the DCPS issue its shutdown command sufficiently far before hitting an operating limit to avoid actually hitting and exceeding it. It turns out that after a protective action command is issued some critical variables can get worse before getting better. Thus, there is a possibility that an operating limit may be reached and exceeded after a DCPS command is issued. To avoid this possibility the DCPS must anticipate worst-case post-protective action transients. In turn, this requires that every 1 millisecond DCPS cycle must include a time-dependent evaluation of limiting scenarios.

Understanding the transition to a safe shutdown state requires a brief description of the NSTX power system, which remains from the earlier TFTR experiment. Each of 37 thyristor rectifiers includes two six-pulse phase-controlled Graetz bridge circuits separately powered through delta and wye windings of a rectifier transformer, with each bridge producing a dc output current of up to 24 kA at a voltage that is controllable within a ± 1 kV range by thyristor firing angle delay adjustments made by a control computer. All 74 rectifier bridge outputs are dc-isolated from each other which allows their controlled dc outputs to be interconnected as needed to drive separately controllable currents in each of the 12 PF coil circuits, in the single OH coil circuit, and in the single TF coil circuit. Connected in parallel with each rectifier bridge circuit is a shorting "bypass" leg of thyristors. The hardwired safety controls for the power system implement a "Level 1 Fault" response for equipment protection safety in which the repetitive firing of bridge thyristors is blocked while the bypass thyristors are fired, effectively inserting a zero voltage short across the coil circuit terminals. This Level 1 fault response can be externally commanded from outside the power system and will be commanded by the DCPS to initiate a shutdown when needed. After a random delay of up to 4.25 milliseconds currents will decline to zero over a much longer time due to energy dissipation in coil circuit resistances.

Critical variables can increase even with the Level 1 Fault condition asserted, for three reasons. First, coil current will continue to resistively heat coils, so all coil temperatures will continue to increase after a DCPS command is issued. Second, the mutual inductance coupling of coil currents to each other can allow the resistive decay of currents in some coils to cause currents in strongly coupled other coils to transiently increase, thus increasing forces and stresses. Third, with zero volts applied to all coils the uncontrolled plasma will eventually suffer a full disruption whose inductive coupling can transiently increase certain coil currents and forces.

VI. DCPS ANTICIPATION OF SHUTDOWN AFTERMATH

The strategy taken in the DCPS algorithm to anticipate the aftermath of a shutdown command is to perform special contingent "look-ahead" calculations. Wherever it is possible for critical variables to worsen after protection action is commanded, the DCPS estimates in real-time the maximum peak critical variable values that could be reached, contingent on the assumption that the DCPS immediately issues the shutdown command. Note that in truth the assumed shutdown command will not have been issued when the calculation is made. The actual DCPS shutdown command is then issued if a calculated critical variable peak in the contingent future reaches its operating limit. This strategy guarantees operating limits will not be exceeded after protective action is commanded.

An algorithm implementing this strategy is quite simple for thermal protection of the TF coil. Energy stored in its magnetic field is the square of TF coil current times half the TF inductance. The algorithm adds a constant multiple of this stored TF magnetic energy to the simulated TF conductor temperature to calculate its final temperature in the event of a shutdown command. This projected contingent peak temperature is then compared to its operating limit to decide whether to issue the command. The algorithm for thermal protection of OH and PF coils is more complicated due to the magnetic coupling that links their currents. Allocation of total PF magnetic energy to individual coils is based on mutual inductances and circuit resistances. The projected final temperature of each coil is then calculated as for the TF coil.

To evaluate post-shutdown increases of coil currents, forces, and/or stresses, there is no alternative to numerically solving the coupled system of differential equations governing evolution of toroidally directed currents, i.e.,

$$\frac{d}{dt} \begin{pmatrix} \frac{M_{coils}}{M'_{coils:eddy}} & \frac{M_{coils:eddy}}{M_{eddy}} & \frac{M_{coils:pl}}{M_{eddy:pl}} \\ \frac{M'_{coils:eddy}}{M'_{coils:pl}} & \frac{M_{eddy}}{M'_{eddy:pl}} & L_{pl} \end{pmatrix} \begin{bmatrix} I_{coils} \\ I_{eddy} \\ I_{pl} \end{bmatrix} + \begin{bmatrix} R_{coils} & \underline{0} & \underline{0} \\ \underline{0} & R_{eddy} & \underline{0} \\ \underline{0}' & \underline{0}' & R_{pl} \end{bmatrix} \begin{bmatrix} I_{coils} \\ I_{eddy} \\ I_{pl} \end{bmatrix} = \begin{bmatrix} V_{coils} \\ \underline{0} \\ \underline{0} \end{bmatrix} \quad (4)$$

Here, \underline{I} vectors represent toroidally directed currents, \underline{V} represents a vector of the galvanically applied power supply voltages which directly drive coil currents, \underline{R} represents diagonal matrices of electrical resistances, \underline{M} represent inductance matrices, and L represents a single inductance. Subscripts reference coils, eddy currents, or plasma (pl). Eddy currents are included for better accuracy.

Inductance values involving only coils or other metallic components are constant due to their fixed geometry, so may be passed through the time derivative operator in Eq.(4). Inductance and resistance values involving the plasma are variable, and require other models in addition to Eq.(4). Because of this distinctive aspect of the plasma it is useful to separate variable-geometry plasma quantities from fixed-geometry quantities. Setting coil circuit voltages to zero to represent a contingent post-shutdown DCPS simulation, get:

$$\begin{bmatrix} \frac{M_{coils}}{M'_{coils:eddy}} & \frac{M_{coils:eddy}}{M_{eddy}} \end{bmatrix} \begin{bmatrix} \dot{I}_{coils} \\ \dot{I}_{eddy} \end{bmatrix} + \begin{bmatrix} R_{coils} & \underline{0} \\ \underline{0} & R_{eddy} \end{bmatrix} \begin{bmatrix} I_{coils} \\ I_{eddy} \end{bmatrix} = - \frac{d}{dt} \begin{bmatrix} M_{coils:pl} \\ M_{eddy:pl} \end{bmatrix} I_{pl} \quad (5)$$

Eqs.(5) is simplified further with its right side becoming zero if the plasma's current and geometry remained constant, as is justified below for limiting DCPS algorithm scenarios. Its numerical evaluations could be even further simplified by the system's approximate linearity which becomes exact if one ignores resistance changes with metal temperatures. Since coil circuit voltages become zero upon DCPS issuance of a shutdown command, the remaining system to solve numerically would then be as follows:

$$\begin{bmatrix} \dot{I}_{coils} \\ \dot{I}_{eddy} \end{bmatrix} = - \left(\begin{bmatrix} \frac{M_{coils}}{M'_{coils:eddy}} & \frac{M_{coils:eddy}}{M_{eddy}} \end{bmatrix}^{-1} \begin{bmatrix} R_{coils} & \underline{0} \\ \underline{0} & R_{eddy} \end{bmatrix} \right) \begin{bmatrix} I_{coils} \\ I_{eddy} \end{bmatrix} \quad (6)$$

The solution to Eq. (6) simply multiplies the initial vector of currents by a state transition matrix determined in advance. This projects the currents forward through a fixed time interval. Repeating this leads to a sequence of current vector projections. Force and stress sequences are next determined by applying Eqs. (2) and (3) to this current vector sequence. Approximate peaks of current, force and stress are then found by direct examination of the sequences. Actual peaks occurring between samples are calculated via quadratic interpolation from the nearest neighbors of the sequential sample peaks.

VII. PLASMA CURRENT WAVEFORM UNCERTAINTY

Feedback control of the plasma is halted by the zero voltages a DCPS shutdown command applies to all coil circuits. The plasma will disrupt as a result, reducing plasma current to zero. Unfortunately, the timing of this plasma disruption within the DCPS' simulated contingent future is completely uncertain, making it impossible to simulate it.

The DCPS strategy for addressing the plasma current waveform uncertainty after an assumed shutdown command is to separately analyze two limiting plasma disruption scenarios. Actual disrupting plasma current will not increase from its initial value to an even greater current, nor will it overshoot to reach negative values. Thus, the first plasma current disruption scenario leaves the plasma current constant at its initial value, unchanged throughout a simulation of contingent post-protection coil currents. It serves as a limiting upper bound for plasma current vs. contingent time. The second scenario has the plasma immediately disrupting, with plasma current dropping to zero as a step function at the simulation's start. This second scenario serves as a plasma current lower bound.

This choice of limiting plasma scenarios has the practical benefit that plasma current changes do not occur during either DCPS simulation; this justifies ignoring plasma changes as discussed earlier so that Eq.(6) with its solution applies.

VIII. EDDY CURRENT MODEL

It turns out that ignoring eddy currents leads to the prediction of excessive currents and forces associated with plasma disruptions. Thus, eddy currents are included in order to reduce unnecessary conservatism.

For the scenario with no change in plasma current, Eq.(6) is solved using the present current vector as its initial state. For the scenario with the initial plasma disruption, the initial state must also include the flux-conserving change to currents produced by an initial full plasma disruption, as follows:

$$\begin{bmatrix} I_{coils}(t_0^+) \\ I_{eddy}(t_0^+) \end{bmatrix} = \begin{bmatrix} I_{coils}(t_0^-) \\ I_{eddy}(t_0^-) \end{bmatrix} + \begin{bmatrix} M_{coils} & M_{coils:eddy} \\ M_{coils:eddy} & M_{eddy} \end{bmatrix}^{-1} \begin{bmatrix} M_{coils:pl} \\ M_{eddy:pl} \end{bmatrix} I_{pl}(t_0^-) \quad (7)$$

Instead of modeling eddy currents as a collection of individual currents flowing in many discrete ring elements, it is useful to perform an eigenmode analysis to find a more convenient linear basis. In the eigenmode basis both inductance and resistance matrices of eddy currents are diagonal.

Fig.8 plots the NSTX passive conducting structures in the poloidal half-plane, superimposed on cross sections of the PF and OH coils. To analyze eddy currents in these, the conducting structures were subdivided into 1378 ring elements, their inductance and resistance matrices were calculated, an eigenmode analysis of the matrices was carried out, and the mutual inductances and force influence coefficients between the eigenmode current patterns and the coils and plasma were also calculated. Eigenmode current patterns have the orthogonality properties that (1) each has its own characteristic exponential decay time constant, (2) they are not inductively coupled to each other, and (3) any pattern of currents in the passive conducting structure can be uniquely represented as a sum of eigenmode current patterns. Fig.9 plots the spectrum of decay time constants for the slowest hundred of these eigenmodes, which range from 21 to 0.3 milliseconds.

In order for the DCPS to evaluate the contingent simulations including eddy current effects, it must have initial

values for $I_{eddy}(t_0^-)$, the vector representing eddy currents flowing in passive structures at the "present" time. This is different from the situation for coil currents which are provided to the DCPS as a set of real-time measurements, since there is no sensing system to measure the eddy currents. Instead, the DCPS will implement an "observer" algorithm to estimate the eddy currents in real-time using their known dynamic model.

This observer algorithm solves the following differential equation system in real-time for a time-varying vector, \underline{y} , which has the same number of components as are retained in the model to represent eddy currents:

$$\underline{M}_{eddy} \dot{\underline{y}} + \underline{R}_{eddy} \underline{y} = \underline{M}_{coils:eddy} \underline{I}_{coils} + \underline{M}_{plasma:eddy} I_{pl} \quad (8)$$

then it updates its estimate of the eddy currents as follows:

$$\hat{I}_{eddy} = \left(\underline{M}_{eddy} \right)^{-1} \left(\underline{R}_{eddy} \underline{y} - \underline{M}_{coils:eddy} \underline{I}_{coils} - \underline{M}_{plasma:eddy} I_{pl} \right) \quad (9)$$

Deviations between this observer algorithm estimate and the actual eddy current vector decay to zero with the time constants of the eigenmodes themselves.

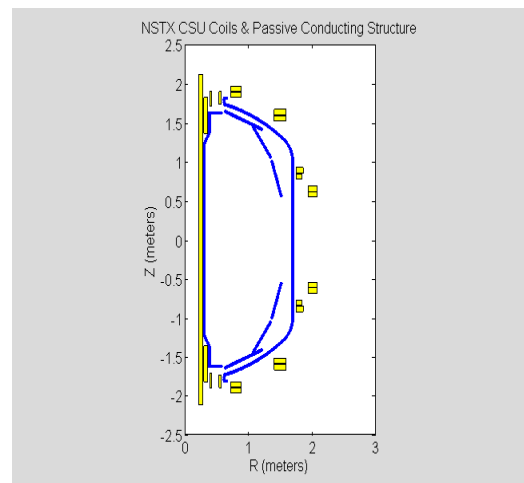


Figure 8: NSTX Coupled Passive Conductors and Coils

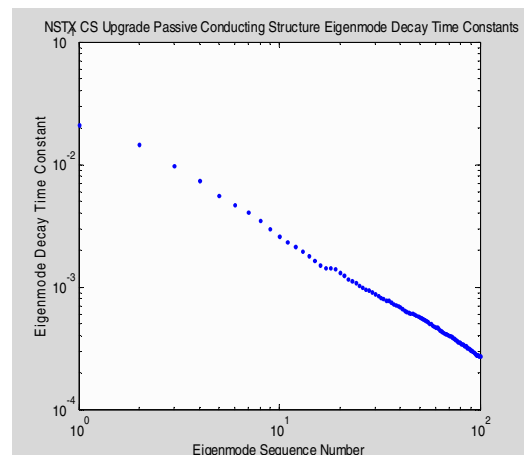


Figure 9: Eigenmode Decay Time Constant Spectrum

Fig.10 plots the OH and PF coil currents calculated for three shutdown simulations, one modeling only the coils without passive conducting structures, one modeling the coils with 100 retained eigenmodes representing conducting structure eddy currents, and the third with 10 eigenmodes modeled. All three are contingent on a shutdown command at time $t=0$ and a 2 MA abrupt plasma disruption delayed for clarity to $t=5$ milliseconds. Inspection shows that either the 10 or the 100 eigenmode simulations would eliminate the excessive conservatism of ignoring eddy currents altogether.

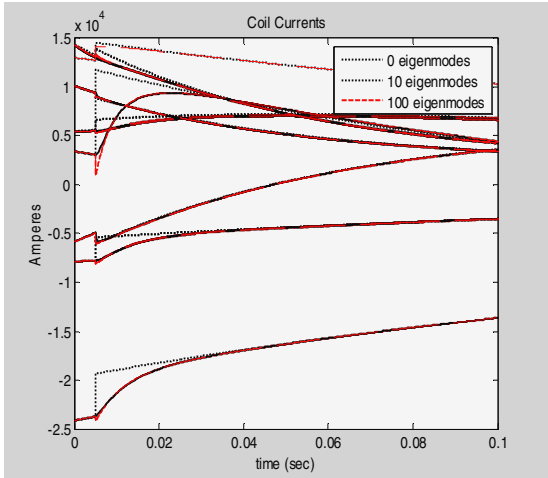


Figure 10: Coil currents after DCPS shutdown command, with plasma disruption, calculated with 100, 10, and 0 eigenmodes modeled

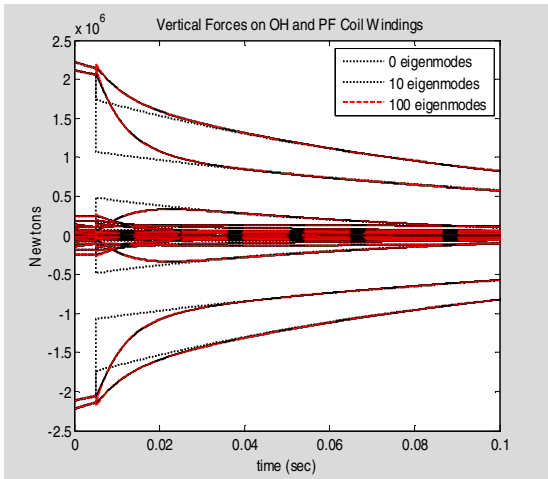


Figure 10: Coil vertical forces after DCPS shutdown command, with plasma disruption, calculated with 100, 10, and 0 eigenmodes modeled

IX. REDUNDANCY

To meet high reliability goals, the DCPS will be implemented by two separate electronic boxes. Since current monitoring signals used by the DCPS are also used for servo-feedback control of plasma and coils' currents, each current monitoring sensor input to DCPS will be provided twice to each DCPS box, i.e., from two entirely separate sets of redundant current sensors. In this way, no single-point failure can both cause a dangerous condition through the feedback control system and also defeat protection action. DCPS algorithms will include automatic cross checking between the redundant current sensor input signals it monitors, issuing a shutdown command if corresponding current signals differ by more than a small allowable discrepancy.

X. DCPS SYSTEMS CODE

A "Systems Code" of DCPS algorithms is being developed to identify any problems in DCPS algorithms before completion of the NSTX Centerstack upgrade so that they can be addressed before the DCPS must be operational. One presently unresolved issue is whether plasma position information should also be input in order that DCPS algorithms might more accurately estimate the mutual inductance and force influence coefficients of the plasma on coils; this would support reductions in conservatism in the choice of plasma coefficients, further expanding the safe operating region.

XI. CONCLUSIONS

The NSTX CS Upgrade is implementing a digital coil protection system (DCPS) to enforce critical variable operating limits in real-time. The DCPS will permit access to essentially regions of potential operating space which are safe for equipment while preventing operations beyond safe operating limits. The DCPS is being pursued as a less expensive approach to the alternative of mechanically overdesigning the coils and structural support systems. DCPS development is now focusing on the detailed design and subsequent performance evaluations of its protection algorithms.

REFERENCES

- [1] P. H. Titus, R. D. Woolley, R. Hatcher, "Stress Multipliers for the Nstx Upgrade Digital Coil Protection System", Proceedings of the 24th Symposium on Fusion Engineering, 26-30 June 2011, Chicago, Illinois

The Princeton Plasma Physics Laboratory is operated
by Princeton University under contract
with the U.S. Department of Energy.

Information Services
Princeton Plasma Physics Laboratory
P.O. Box 451
Princeton, NJ 08543

Phone: 609-243-2245
Fax: 609-243-2751
e-mail: pppl_info@pppl.gov
Internet Address: <http://www.pppl.gov>